Soft Matter

PAPER

View Article Online
View Journal | View Issue

Cite this: *Soft Matter*, 2024, **20**, 7030

Ellipsoidal micelle formation of quaternary ammonium salt-based gemini surfactants: structural analysis through small-angle X-ray scattering

Tsukasa Morita,[a] Shiho Yada[b] and Tomokazu Yoshimura *[a]

Gemini surfactants exhibit better adsorption and aggregation properties than those of monomeric surfactants. However, to enhance the functional properties of gemini surfactants, the effect of spacer structures on their aggregation behavior must be elucidated. Small-angle X-ray scattering (SAXS) has been performed to study the aggregate structures of monomeric surfactants, but its application has not been expanded to the analysis of gemini surfactants. Therefore, in this study, we performed a structural analysis of aggregates formed by quaternary ammonium salt-based gemini surfactants with different spacer structures in aqueous solutions through viscosity, dynamic light scattering (DLS), and SAXS measurements. We also investigated the effects of the spacer structure and surfactant concentration on the aggregation behavior. The DLS results indicated that gemini surfactants with spacers containing cyclic structures, such as diethylene and triethylene chains, formed small micelles (several nanometers in size) at the limiting concentration for dissolution in water. In contrast, gemini surfactants with nitrogen and oxygen atoms at the center of the spacer formed ellipsoidal micelles at low concentrations, as shown by SAXS results. The core and overall radii of the minor and major axes of the ellipsoidal micelles decreased with increasing surfactant concentration and were larger for spacers with two ethylene chains connected to central nitrogen and oxygen atoms than for spacers with rigid diethylene and ethylene chains connected to a central nitrogen atom.

Received 24th March 2024,
Accepted 12th August 2024

DOI: 10.1039/d4sm00342j

rsc.li/soft-matter-journal

Introduction

Small-angle X-ray scattering (SAXS) can be performed to investigate the structure and size of aggregates formed by surfactants. By measuring the X-rays scattered by a solution of surfactants, detailed structural information on the nanometer order of the aggregates can be obtained. For example, Buhler *et al.* reported that perfluorooctylbutane trimethylammonium bromide, a cationic surfactant, self-assembles into narrow ribbons with average dimensions of 4 nm × 3 nm through SAXS and cryogenic transmission electron microscopy (cryo-TEM).[1] In addition, N^{ε}-acyl lysine methyl ester hydrochloride, a cationic surfactant, exhibits strong thermotropic liquid crystalline behavior because of the structure and positive charge of the molecule.[2] Further, Pérez *et al.* investigated the structures of liquid crystals formed by arginine-based cationic surfactants through SAXS and found that the structures were affected by the hydration of the hydrophilic group.[3] In addition, structural analyses of the aggregates formed by double-chain-type surfactants,[4,5] gemini surfactants,[6,7] mixtures of surfactants and polymers,[8–10] and nanoparticles[11,12] have been performed through SAXS. SAXS is a useful technique for the structural analysis of aggregates formed by surfactants; however, to evaluate if the analysis is correct, it is necessary to combine and support multiple techniques such as rheology, dynamic light scattering (DLS), and cryo-TEM observations.

Recently, oligomeric surfactants with multiple hydrophobic and hydrophilic groups have been developed as a new class of surfactants with improved properties and functionalities in relation to those of conventional monomeric surfactants. Among these, gemini surfactants with two hydrophobic and two hydrophilic groups, which are structurally connected to monomeric surfactants *via* spacers at or near the hydrophilic groups, exhibit excellent surface activity, as evidenced by their lower critical micelle concentration (CMC) and higher surface-tension-reducing abilities than those of the corresponding monomeric surfactants. Gemini surfactants also exhibit unique aggregation behavior in aqueous solutions. For example, Zana *et al.* investigated the aggregation behavior of quaternary

[a] *Department of Chemistry, Faculty of Science, Nara Women's University, Kitauoyanishi-machi, Nara 630-8506, Japan. E-mail: yoshimura@cc.nara-wu.ac.jp*
[b] *Department of Industrial Chemistry, Faculty of Engineering, Tokyo University of Science, 6-3-1 Niijuku, Katsushika-ku, Tokyo 125-8585, Japan*

ammonium salt-based gemini surfactants of alkanediyl-α,ω-bis-(dimethylalkylammonium bromide) ($2C_n$-s, where n and s represent the alkyl and spacer alkylene chain lengths, respectively).[13,14] Notably, $2C_n$-s forms spherical micelles at concentrations close to the CMC, independent of the alkyl and spacer chain lengths. Of note, $2C_{12}$-s with s = 3, 4, and 5 showed significant micellar growth, and those with s = 6, 8, and 10 formed small micelles over a broad concentration range. Gemini surfactants with short spacers can easily form aggregates with higher-order structures. In addition, sulfonate-type anionic gemini surfactants with two aromatic rings near hydrophilic groups form multilamellar vesicles consisting of several small vesicles owing to intermolecular π–π interactions formed by the aromatic rings.[15] Chiral and achiral cationic gemini surfactants form elongated worm-like micelles in aqueous solutions, and their aggregation behavior is affected by their stereochemistry.[16] To date, we have designed and synthesized novel gemini surfactants having various structures and reported their adsorption and aggregation properties.[17–26] For example, the structures of worm-like micelles formed by a fluorocarbon–hydrocarbon-type hybrid gemini surfactant in aqueous solutions were investigated through SAXS and viscoelastic measurement. The results revealed that increasing the number of entanglements and contour length of the hybrid gemini surfactant resulted in a higher viscosity.[22] Thus, by changing the structure of the hydrophobic group, hydrophilic group, spacer chain length, and functional group connected to the hydrophilic group of the gemini surfactant, unique aggregation behavior can be achieved, which is not observed in conventional surfactants.

Furthermore, we have designed and synthesized novel gemini surfactants having spacers containing cyclic structures such as diethylene and triethylene chains and atoms such as nitrogen and oxygen as well as studied their solution properties.[23–25] Gemini surfactants with flexible spacers containing nitrogen and oxygen atoms are highly soluble in water, whereas those with rigid spacers containing diethylene or triethylene chains are poorly soluble in water. In addition, the adsorption and orientation of the gemini surfactants at the air/water interface are significantly affected by the spacer structure, especially its length.

Although the structural analysis of the aggregates formed by surfactants through SAXS has been widely conducted,[1–16,22] there are only a few reports on the structural analysis of gemini surfactants through SAXS.[6,7,22,23] Clarifying the relationship between the molecular structure of surfactants containing a gemini structure and their aggregation behavior will promote the development of surfactants with high performance and advanced functionalities, particularly in fields such as cosmetics and daily necessities.

In this study, we performed a structural analysis of aggregates formed by quaternary ammonium salt-based gemini surfactants with spacers having cyclic structures such as diethylene and triethylene chains and atoms such as nitrogen and oxygen, denoted $2C_{12}$(Spacer); the structures and abbreviations of $2C_{12}$(Spacer) are shown in Fig. 1. Our investigations included varying the spacer structures and concentration of $2C_{12}$(Spacer), and studying the corresponding changes through rheology analysis, DLS, and SAXS.

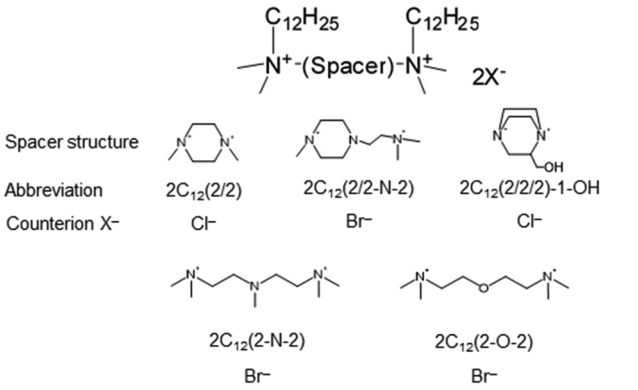

Fig. 1 Structures and abbreviations of the quaternary ammonium salt-based gemini surfactants with different spacer structures ($2C_{12}$(Spacer)).

Material and methods

Materials

Gemini surfactants $2C_{12}$(Spacer) were synthesized by a previously reported method.[23] The spacer structures of the gemini surfactants and CMCs determined *via* conductivity measurement are summarized in Table 1. The gemini surfactant solutions were prepared using Milli-Q Plus water (resistivity = 18.2 MΩ cm; Darmstadt, Germany).

Measurements

The rheological measurement of the gemini surfactants with different spacer structures was performed using a stress-control rheometer (MCR-302; Anton Paar, Graz, Austria) with a cone plate radius of 49.98 mm and cone angle of 1.002°. In the steady flow viscosity measurement mode, the shear rate was varied from 0.01 to 1000 s^{-1}. DLS was performed using an ALV-5000E spectrophotometer (Hessen, Deutschland) equipped with a He–Ne laser (λ = 632.8 nm). For spherical particles, the diffusion coefficient determined by the constrained regularized (CONTIN) method was converted to the apparent hydrodynamic radius (R_H) using the Stokes–Einstein relationship:[26] $D_0 = kT/6\pi\eta R_H$, where D_0 is the diffusion coefficient extrapolated to zero concentration, k is the Boltzmann constant, T is the absolute temperature, and η is the viscosity of the solvent. SAXS was conducted using a SAXS instrument installed on the BL40B2 beamline at SPring-8 (Hyogo, Japan). The X-ray wavelength was set at 0.7 Å. A large-area pixel detector (PILATUS 2M, DECTRIS Ltd, Baden, Germany) with a sample-to-detector distance of 2.0 m was used. The exposure time was 3 min and the scattering vector (q) ranged from 0.3 to 4.0 nm^{-1}. Vector q was determined as follows: $q = (4\pi/\lambda)\sin(\theta/2)$ (where λ and θ are the wavelength and scattering angle, respectively). All measurements were performed at 25.0 ± 0.5 °C.

Model fitting analysis of SAXS

A model-fitting analysis of the SAXS profile was performed to investigate the structures and sizes of the micelles formed by $2C_{12}$(Spacer) in aqueous solutions. Scattering intensity $I(q)$ for the SAXS profile of the micelle solution can be expressed by

Table 1 Gemini surfactant labels, spacer structures, and CMCs

Gemini surfactant label	Spacer structure	CMC/mmol dm^{-3}
$2C_{12}$(2/2)	*N*,*N*′-Dimethylpiperazine	0.320
$2C_{12}$(2/2-N-2)	1-Methyl-4-[2-(*N*,*N*-dimethylammonio)ethyl]piperazine-1-ium	1.40
$2C_{12}$(2/2/2)-1-OH	2-Hydroxymethyl-1,4-diazabicyclo[2,2,2]octane	0.310
$2C_{12}$(2-N-2)	*N*-Methyl-*N*,*N*-bis[2-(*N*′,*N*′-dimethylammonio)ethyl]amine	0.985
$2C_{12}$(2-O-2)	Bis[2-(dimethylammonio)ethyl]ether	1.03

multiplying form factor $P(q)$ by structure factor $S(q)$, as given by eqn (1).

$$I(q) = N_P P(q) S(q) \quad (1)$$

Here, N_P, $P(q)$, and $S(q)$ are the number density of particles, form factor, and structure factor, respectively.[27] $P(q)$ is the average scattering profile of a single particle derived from a geometric model, and $S(q)$ is the interaction between the particles in the solution.[28,29] For the aggregates formed by gemini surfactants, the core–shell ellipsoid model is form factor $P(q)$ of a core–shell ellipsoid with core radius of major axis R_{c1}, core radius of minor axis R_{c2}, shell thickness of major axis T_{s1}, and shell thickness of minor axis T_{s2}:

$$P(q) = 9\int_0^1 \left[\Delta\rho_s V_{tot}\frac{j_1(qr_{tot})}{qr_{tot}} + (\Delta\rho_c - \Delta\rho_s)V_c\frac{j_1(qr_c)}{qr_c}\right]^2 d\mu \quad (2)$$

where $j_1(x)$ is the first-order spherical Bessel function of x, $\Delta\rho_c$ and $\Delta\rho_s$ are the scattering contrasts of the core and shell, respectively, and V_{tot} and V_c are the total volume of the micelle and the volume of the core, respectively. Terms r_{tot} and r_c are defined by eqn (3) and (4), respectively.

$$r_{tot} = [(R_{c1} + T_{s1})^2(1 - \mu^2) + (R_{c2} + T_{s2})^2\mu^2]^{1/2} \quad (3)$$

$$r_c = [R_{c1}{}^2(1 - \mu^2) + R_{c2}{}^2\mu^2]^{1/2} \quad (4)$$

The μ is the cosine of the angle between the vector q and the direction of the minor axis for the oblate model. The axis ratio ν of the ellipsoidal micelles was calculated by dividing the radius of the major axis R_1 ($R_1 = R_{c1} + T_{s1}$) by the radius of the minor axis R_2 ($R_2 = R_{c2} + T_{s2}$). When surfactants form spherical micelles in an aqueous solution, the value of ν is 1.

In anisotropic particles such as ellipsoids, structure factor $S'(q)$ must be modified to account for the anisotropic shape. The interparticle structure factor ($S_{HP}(q)$) for a charged micelle system interacting through a repulsive screened Coulomb potential is given using by rescaled mean spherical approximation, as given by eqn (5).[30,31]

$$S_{HP}(q) = \frac{1}{1 - 24\phi a(q\sigma)} \quad (5)$$

Here, φ is the volume fraction, σ is the effective particle diameter, and $a(q\sigma)$ was obtained from the work of Hayter and Penfold.[30] Note that $a(q\sigma)$ depends on the volume fraction and the degree of ionization and gives the value of Debye length (l_d). l_d is determined by eqn (6):

$$l_d = \left(\frac{\varepsilon\varepsilon_0 kT}{2N_A e^2 I}\right) \quad (6)$$

Here, ε is the dielectric constant of the solvent, ε_0 is the permittivity of free space, N_A is the Avogadro constant, e is the electronic charge, and I is the ionic strength of the solution. For asymmetric particles such as ellipsoidal particles, the structure factor $S'(q)$ is modified to account for the anisotropic shape, as given by eqn (7).[32]

$$S'(q) = 1 + \frac{|\langle F(q)\rangle|^2}{\langle |F(q)|\rangle^2}(S_{HP}(q) - 1) \quad (7)$$

Here, $F(q)$ is the scattering amplitude of the particle and $S'(q)$ is used for model fitting analysis.[32] In this study, we performed a fitting analysis of the SAXS profiles using the oblate core–shell ellipsoid model[32,33] for the micelles formed by $2C_{12}$(2/2-N-2), $2C_{12}$(2-N-2), and $2C_{12}$(2-O-2).

Results and discussion

Rheology

Fig. 2 shows the shear-rate dependence of the viscosity of $2C_{12}$(Spacer). The viscosities of $2C_{12}$(Spacer) differed significantly according to the spacer structure and surfactant concentration. The viscosities of $2C_{12}$(2/2), $2C_{12}$(2/2-N-2), and $2C_{12}$(2/2/2)-1-OH with cyclic structures, *i.e.*, the diethylene and triethylene chains, in the spacer were almost the same as that of water, independent of the surfactant concentration. To clarify the structures of the aggregates, cryo-TEM observations of aqueous solutions of gemini surfactants with cyclic structures were performed; however, the structures of the aggregates could not be clearly captured. We believe that no images could be obtained because of the small sizes of micelles in the low-viscosity micelle solutions. This suggests the formation of small micelles in aqueous solutions. Further, the DLS results showed that the micelles with a size of several nanometers were detected (Fig. 3), which is consistent with the viscosity measurement results. In contrast, the trend of the viscosities of $2C_{12}$(2-N-2) and $2C_{12}$(2-O-2), with nitrogen and oxygen atoms at the center of the spacer, was different from that observed for $2C_{12}$(2/2), $2C_{12}$(2/2-N-2), and $2C_{12}$(2/2/2)-1-OH. The viscosity behavior of these surfactants is highly dependent on the surfactant concentration. For $2C_{12}$(2-N-2), the viscosities at concentrations 10, 25, 50, and 100 times the CMC were almost the same as that of water. However, the viscosity increased as the concentration increased to 200 times the CMC, and an increase in the concentration to 300 and 400 times the CMC further increased the viscosity.

Fig. 4 shows the plots of storage modulus G', which is an elastic term, and loss modulus G'', which is a viscous term, as a

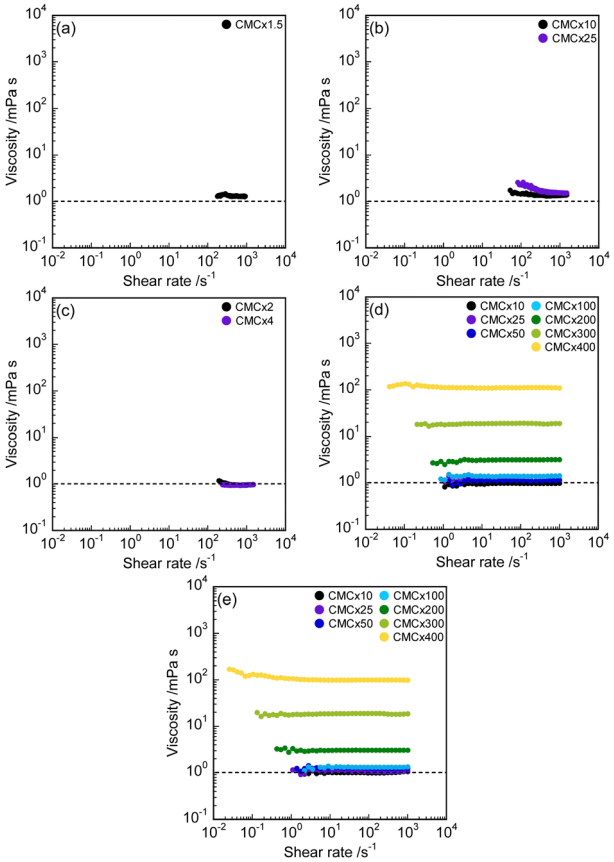

Fig. 2 Shear-rate dependence of viscosity for (a) $2C_{12}$(2/2), (b) $2C_{12}$(2/2-N-2), (c) $2C_{12}$(2/2/2)-1-OH, (d) $2C_{12}$(2-N-2), and (e) $2C_{12}$(2-O-2). Dotted lines represent the viscosity of water.

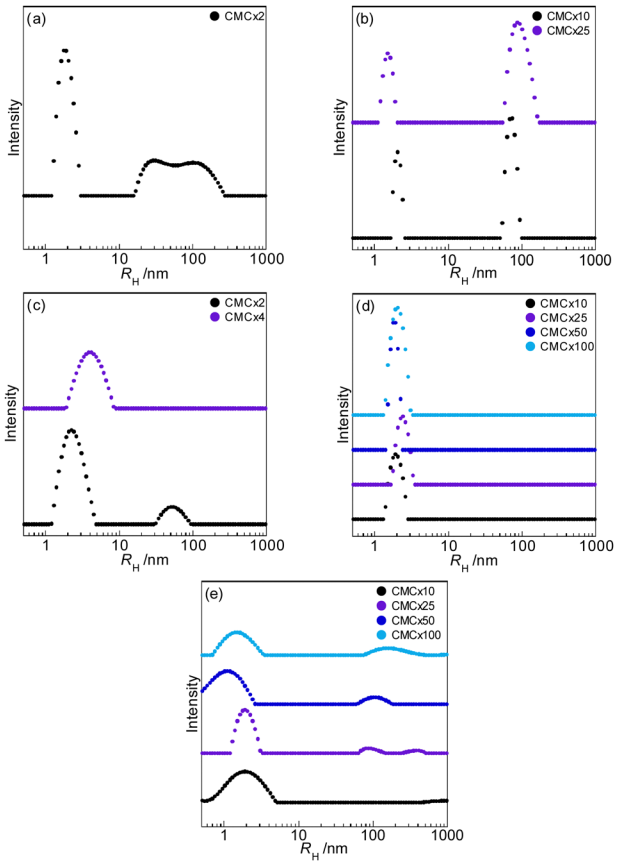

Fig. 3 Size distribution of apparent hydrodynamic radius (R_H) for gemini surfactants: (a) $2C_{12}$(2/2), (b) $2C_{12}$(2/2-N-2), (c) $2C_{12}$(2/2/2)-1-OH, (d) $2C_{12}$(2-N-2), and (e) $2C_{12}$(2-O-2).

function of angular frequency ω at a concentration 200, 300 and 400 times the CMC for $2C_{12}$(2-N-2) and $2C_{12}$(2-O-2). For $2C_{12}$(2-N-2), G'' was higher than G' in all ω regions, a viscous liquid sample. Thus, upon increasing the concentration of $2C_{12}$(2-N-2), the micelle solution was transformed into a viscous one, which can be ascribed to an increase in the number or the growth of the micelles. $2C_{12}$(2-O-2) exhibited viscosity and viscoelasticity behaviors similar to those of $2C_{12}$(2-N-2). $2C_{12}$(2/2-N-2) formed small micelles at low concentrations in aqueous solutions, as mentioned above; however, for $2C_{12}$(2-N-2) and $2C_{12}$(2-O-2) with the same spacer length, the micelle solution was transformed to a viscous one as the surfactant concentration increased. $2C_{12}$(2/2-N-2) has higher rigidity and is a more hydrophobic spacer than $2C_{12}$(2-N-2) and $2C_{12}$(2-O-2) because of the rigid diethylene chain in the spacer, resulting in the formation of small micelles. The gemini surfactant with pentylene spacer $2C_{12}$-5 showed significant micelle growth with increasing surfactant concentration.[13] Despite the change in the spacer from $2C_{12}$-5 to $2C_{12}$(2-N-2) and $2C_{12}$(2-O-2), which have the same spacer length, similar aggregation behavior was observed, despite the presence of nitrogen and oxygen atoms, respectively, at the center of the spacer. Thus, the aggregation behavior of gemini surfactants was confirmed to be significantly affected by the spacer structures. The rigid diethylene chain in the spacer gives rise to the formation of small micelles.

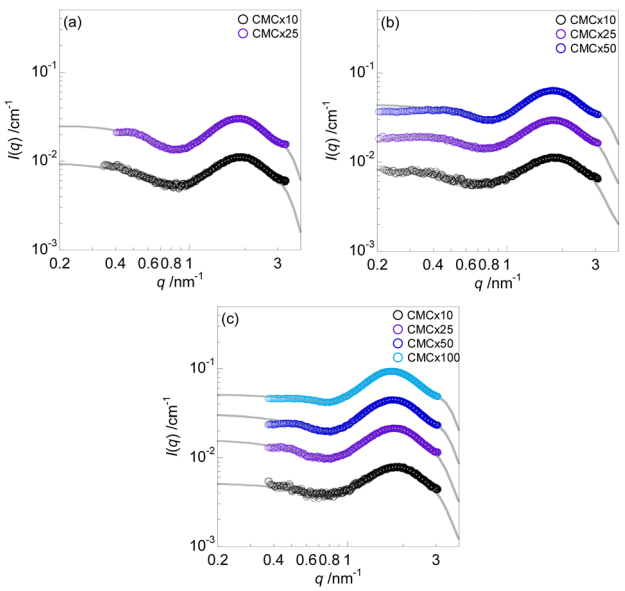

Fig. 4 SAXS data and fitting curves for (a) $2C_{12}$(2/2-N-2), (b) $2C_{12}$(2-N-2), and (c) $2C_{12}$(2-O-2). Solid lines represent the best-fit theoretical scattering functions.

Structural analysis of micelles *via* SAXS

The structures of the micelles formed by gemini surfactants $2C_{12}$(Spacer) in aqueous solutions, which exhibited the same low viscosity as that of water, were investigated in detail through SAXS. Fig. 5 shows the SAXS profiles of $2C_{12}$(2/2-N-2), $2C_{12}$(2-N-2), and $2C_{12}$(2-O-2) with the best-fit theoretical scattering curves obtained using eqn (2). For $2C_{12}$(2/2) and $2C_{12}$(2/2/2)-1-OH, SAXS could not be performed because of the low scattering intensities arising from the low surfactant concentrations, which are the limits of dissolution in water. For $2C_{12}$(2-N-2) at a concentration 100 times the CMC, the best-fit theoretical scattering could not be obtained. The SAXS profiles of $2C_{12}$(Spacer) showed a flat region ($I(q)_0$) in the low-q range, with a decrease in the scattering intensity at q = 0.4–0.5 nm^{-1}. This indicates that the formed aggregates were small micelles. As the surfactant concentration was increased, a peak was observed at q = 0.4–0.5 nm^{-1}, which can be ascribed to the electrostatic repulsion between the micelles and is related to $S(q)$.[22,34] The peak at q = 1.7–1.8 nm^{-1} is associated with the difference in the scattering length density between the hydrophobic and hydrophilic regions in the micelle, indicating that the micelles have a core–shell structure.

The SAXS profiles of the gemini surfactants were fitted using a core–shell ellipsoid model. Table 2 lists the apparent hydrodynamic radii obtained from DLS, the core radii of the major and minor axes (R_{c1} and R_{c2}), the shell thicknesses of the major and minor axes (T_{s1} and T_{s2}), the overall radii of the major and minor axes (R_1 and R_2), the axis ratio v and aggregation number (N_{agg}) for the ellipsoidal micelles formed by $2C_{12}$(2/2-N-2), $2C_{12}$(2-N-2), and $2C_{12}$(2-O-2). These measurements were obtained through model-based analysis. N_{agg} can be obtained by eqn (8).

$$N_{agg} = \frac{V_{core}}{V_{mon}} \tag{8}$$

Here, V_{core} is the core volume from the fitting analysis and V_{mon} is the alkyl chain volume of the gemini surfactants. $V_{mon} = 2V$ was obtained because the gemini surfactants have two alkyl chains in the molecule. V was calculated using the Tanford equation. V_{core} and V are defined by eqn (9) and (10), respectively.[35,36]

$$V_{core} = \frac{4}{3}\pi {R_{c1}}^2 R_{c2} \tag{9}$$

$$V = (27.4 + 26.9n) \times 10^{-3} \tag{10}$$

Here, n is the number obtained by subtracting one from the number of carbon atoms in the alkyl chains of the gemini surfactant molecules.

The ellipsoid micelle sizes obtained from SAXS were nearly the same as the sizes and distribution obtained from DLS. However, the effect on micelle size with increasing surfactant concentrations was different in both methods. The aggregate sizes obtained using the Stokes–Einstein equation from the autocorrelation function obtained by the DLS measurements were assumed to be consistent with spherical particles; however, model-fitting analysis of the SAXS results indicated that the gemini surfactants formed ellipsoidal micelles, and the size distribution obtained from the DLS was considered to reflect the length anisotropy of the minor and major axes of the ellipsoidal micelles. Therefore, the differences in the size of micelles formed by gemini surfactants are interpreted as differences in the respective measurement methods.

Thus, $2C_{12}$(2/2-N-2), $2C_{12}$(2-N-2), and $2C_{12}$(2-O-2) formed ellipsoidal micelles with v of approximately 2, independent of the spacer structure and surfactant concentration (Table 2). Fig. 6 shows an illustration of the arrangement of molecules in the ellipsoidal micelles formed by gemini surfactants $2C_{12}$(2/2-N-2), $2C_{12}$(2-N-2), and $2C_{12}$(2-O-2) based on previous reports.[37,38] Given the size distribution derived from DLS data, as shown in Fig. 3, the dimensions of the ellipsoidal micelles were found to be similar. The aggregate size, estimated using the Stokes–Einstein equation based on the autocorrelation function from the DLS data, was predicated on a spherical model. However, the gemini surfactants in this study formed ellipsoidal micelles according to the model-fitting analysis of SAXS. Moreover, the size distribution derived from DLS data is considered to reflect the anisotropy of the lengths of the minor and major axes of the ellipsoidal micelles. Surfactants are known to form spherical micelles at low concentrations in aqueous solutions. For example, a gemini surfactant with a pentylene spacer ($2C_{12}$-5) has been reported to form spherical micelles in aqueous solutions.[13] However, $2C_{12}$(2/2-N-2), $2C_{12}$(2-N-2), and $2C_{12}$(2-O-2) have two hydrophobic and two hydrophilic groups; they also have bulky spacer structures in the molecules, which may result in a smaller molecular curvature. Therefore, it is difficult to neatly pack the molecules into the micelles during micelle formation (Fig. 6). Thus, they likely form ellipsoidal rather than spherical micelles. In addition, their R_{c1}, R_{c2}, R_1, and R_2 values decreased with their increasing concentration. In contrast, T_{s1} and T_{s2} negligibly changed for all spacer structures, independent of the

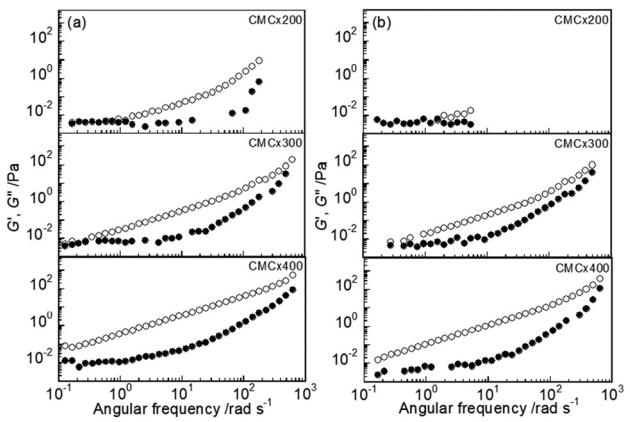

Fig. 5 Frequency dependence of storage and loss moduli (black solid circle, G'; black open circle, G'') for gemini surfactants at concentrations 200, 300, and 400 times the CMC: (a) $2C_{12}$(2-N-2) and (b) $2C_{12}$(2-O-2).

Table 2 Structural parameters obtained from DLS and model fitting analysis of SAXS results for the gemini surfactants

	CMC×	R_H/nm	R_{c1}/nm	R_{c2}/nm	T_{s1}/nm	T_{s2}/nm	R_1/nm	R_2/nm	ν	N_{agg}
$2C_{12}$(2/2-N-2)	10	2.09 ± 0.32	2.01	1.71	2.55	0.646	4.56	2.36	1.93	21
	25	1.56 ± 0.36	1.88	1.69	2.59	0.514	4.48	2.20	2.03	20
$2C_{12}$(2-N-2)	10	2.11 ± 0.71	2.25	2.04	2.81	0.384	5.06	2.42	2.09	34
	25	2.53 ± 0.76	2.07	1.93	2.80	0.364	4.86	2.29	2.12	28
	50	1.87 ± 0.36	1.87	1.68	2.76	0.355	4.64	2.04	2.23	19
$2C_{12}$(2-O-2)	10	2.81 ± 2.06	2.07	1.97	2.68	0.468	4.85	2.41	2.02	29
	25	2.17 ± 0.88	2.04	1.96	2.72	0.467	4.75	2.44	1.96	29
	50	1.45 ± 1.16	1.88	1.76	2.72	0.450	4.60	2.21	2.08	21
	100	2.00 ± 1.30	1.85	1.66	2.70	0.447	4.55	2.11	2.16	19

R_H, apparent hydrodynamic radius; R_{c1}, core radius of the major axis; R_{c2}, core radius of the minor axis; T_{s1}, shell thickness of the major axis; T_{s2}, shell thickness of the minor axis; R_1, radius of the major axis; R_2, radius of the minor axis; ν, axis ratio for ellipsoidal micelles; N_{agg}, aggregation number.

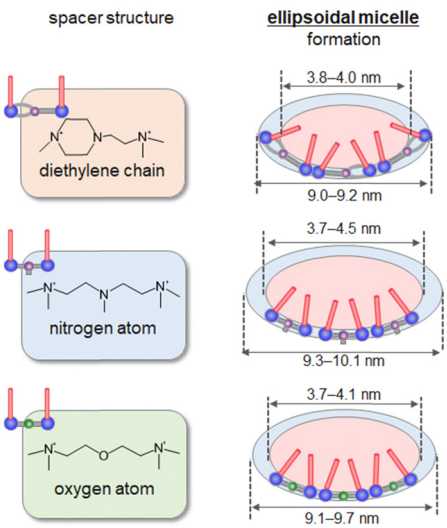

Fig. 6 Illustration of the arrangement of molecules into the ellipsoidal micelles formed by gemini surfactants $2C_{12}$(2/2-N-2), $2C_{12}$(2-N-2) and $2C_{12}$(2-O-2).

concentration. These results reveal that the ellipsoidal micelles formed by the gemini surfactants were more influenced by the core than the shell. The N_{agg} values of the gemini surfactants decreased with increasing surfactant concentration. The N_{agg} of conventional ionic surfactant micelles is approximately 60. However, the gemini surfactants having a two-molecule-based connecting structure had N_{agg} values of less than half of the monomeric surfactants, particularly as the concentration increased. This indicates that the gemini surfactants have bulky spacers that make packing into micelles difficult. The N_{agg} values of gemini surfactants $2C_{12}$(2/2-N-2), $2C_{12}$(2-N-2), and $2C_{12}$(2-O-2) were lower than those of the gemini surfactant having the pentylene spacer $2C_{12}$-5 (N_{agg} = 30–40).[13] It may be challenging to pack the gemini surfactants with nitrogen and oxygen at the center of the spacer into the micelles during micelle formation because they have a bulkier structure than $2C_{12}$-5. The T_{s2} of $2C_{12}$(2/2-N-2) was larger than those of $2C_{12}$(2-N-2) and $2C_{12}$(2-O-2), and T_{s1} was slightly smaller because of the diethylene-chain-containing bulky spacer structure. The R_{c1} and R_{c2} and overall R_1 and R_2 values of these ellipsoidal micelles were larger for $2C_{12}$(2-N-2) and $2C_{12}$(2-O-2) than for $2C_{12}$(2/2-N-2). $2C_{12}$(2/2-N-2) formed smaller ellipsoidal micelles than $2C_{12}$(2-N-2) and $2C_{12}$(2-O-2) because $2C_{12}$(2/2-N-2) has rigid and bulky diethylene chains in the spacer, making it difficult for the molecules to aggregate (Fig. 6). The N_{agg} value of $2C_{12}$(2/2-N-2) was also smaller than those of $2C_{12}$(2-N-2) and $2C_{12}$(2-O-2) at the same concentration, indicating that the molecules of $2C_{12}$(2/2-N-2) could not pack easily into micelles.

Therefore, the size and aggregation number of the micelles formed by gemini surfactants at low concentrations in aqueous solutions are significantly affected by the rigid and flexible structures of the spacer, regardless of the presence of atoms such as nitrogen and oxygen. Our future investigations will focus on pH and temperature to acquire in-depth information on the aggregation properties of the gemini surfactants in aqueous solutions.

Conclusions

The structures of aggregates formed by quaternary ammonium salt-based gemini surfactants containing spacers having cyclic structures, such as diethylene and triethylene chains, and atoms, such as nitrogen and oxygen [$2C_{12}$(Spacer); $2C_{12}$(2/2), $2C_{12}$(2/2-N-2), $2C_{12}$(2/2/2)-1-OH, $2C_{12}$(2-N-2), and $2C_{12}$(2-O-2)] were investigated through rheology analysis, SAXS, and DLS. The effects of the spacer structure and surfactant concentration on the aggregation behavior were examined. The gemini surfactants with spacers containing the cyclic structures, $2C_{12}$(2/2) and $2C_{12}$(2/2/2)-1-OH, formed small micelles at a low concentration when dissolved in water. In contrast, the gemini surfactants with atoms such as nitrogen and oxygen in the center of the spacer, $2C_{12}$(2/2-N-2), $2C_{12}$(2-N-2), and $2C_{12}$(2-O-2), formed ellipsoidal micelles at low concentrations according to model fitting analysis of the SAXS results; the latter two changed from micelle solutions to viscous solutions with increasing concentration. The sizes and aggregation numbers of these ellipsoidal micelles differed according to the spacer structure and surfactant concentration. The core and overall radii of the minor and major axes of the ellipsoidal micelles decreased with increasing

surfactant concentration, and their aggregation numbers decreased. The core and overall radii of the minor and major axes of the ellipsoidal micelles formed by $2C_{12}$(2/2-N-2) were smaller than those by $2C_{12}$(2-N-2) and $2C_{12}$(2-O-2), and the shell thickness was larger because of the bulky spacer structure consisting of a rigid diethylene chain and ethylene linked to the central nitrogen atom of the spacer. In summary, in this study, we elucidated the relationship between the structures of aggregates formed by gemini surfactants with different spacer structures, $2C_{12}$(Spacer), and various structural factors, including spacer structure and surfactant concentration. Because the development of gemini surfactants has been hindered by problems such as their complex synthesis and the high cost of the precursor materials, we aimed to address and mitigate these issues. Specifically, based on the findings of this study, improved gemini surfactants with high performance and advanced functionalities can be developed. Further developments *via* appropriate molecular design and synthesis will render these surfactants suitable for a wide range of industrial applications.

Author contributions

Tsukasa Morita: investigation, writing the original draft, writing the review, and editing. Shiho Yada: investigation, resources, validation. Tomokazu Yoshimura: conceptualization, supervision.

Data availability

Data for this article, including [description of data types] are available at [name of repository] at **https://doi.org/10.1039/D4SM00342J**.

Conflicts of interest

The authors declare that they have no competing financial interests or personal relationships that could have influenced the work reported in this study.

Acknowledgements

We thank Dr Hiroki Iwase and Mrs Misaki Ueda (CROSS) for their support with the use of rheology equipment. Synchrotron radiation experiments were performed at BL40B2 at SPring-8 with the approval of the Japan Synchrotron Radiation Research Institute (JASRI) (proposal No. 2014A1456 and 2014B1502). The authors thank Editage (**https://www.editage.jp**) for the English language editing.

References

1 E. Buhler, C. Oelschlaeger, G. Waton, M. Rawiso, J. Schmidt, Y. Talmon and S. J. Candau, *Langmuir*, 2006, **22**, 2534.
2 A. Mezei, L. Pérez, A. Pinazo, F. Comelles, M. R. Infante and R. Pons, *Langmuir*, 2012, **28**, 16761.
3 L. Pérez, R. Pons, F. F. Oliveira de Sousa, M. del C. Morán, A. Ramos da Silva and A. Pinazo, *J. Mol. Liq.*, 2021, **339**, 116819.
4 Y. Kawabata, K. Hayashi, T. Kanao and A. Ishikawa, *Colloids Surf., A*, 2014, **441**, 140.
5 R. A. Gonçalves, B. Lindman, M. G. Miguel, T. Iwata and Y. M. Lam, *J. Colloid Interface Sci.*, 2018, **528**, 400.
6 Q. Li, M. Yao, X. Yue and X. Chen, *Langmuir*, 2017, **33**, 4328.
7 K. Morishima, S. Sugawara, T. Yoshimura and M. Shibayama, *Langmuir*, 2017, **33**, 6084.
8 Q. Li, X. Yue, P. Shang, Y. Quan, M. Ren, Y. Ma and X. Chen, *Colloids Surf., A*, 2016, **489**, 67.
9 S. G. Trindade, L. Piculell and W. Loh, *Langmuir*, 2022, **38**, 2906.
10 K. J. Clinckspoor, F. B. Okasaki and E. Sabadini, *J. Colloid Interface Sci.*, 2022, **607**, 1014.
11 M. Harada, K. Saijo and N. Sakamoto, *Colloids Surf., A*, 2009, **349**, 176.
12 S. Yada and T. Yoshimura, *Langmuir*, 2019, **35**, 5241.
13 D. Danino, Y. Talmon and R. Zana, *Langmuir*, 1995, **11**, 1448.
14 R. Zana, *J. Colloid Interface Sci.*, 2002, **248**, 203.
15 Z. Hordyjewicz-Baran, J. Woch, E. Kuliszewska, J. Zimoch, M. Libera, A. Dworak and B. Trzebicka, *Colloids Surf., A*, 2015, **484**, 336.
16 M. E. Franke and H. Rehage, *Langmuir*, 2019, **35**, 8968.
17 T. Yoshimura, T. Ichinokawa, M. Kaji and K. Esumi, *Colloids Surf., A*, 2006, **273**, 208.
18 T. Yoshimura, A. Ohno and K. Esumi, *Langmuir*, 2006, **22**, 4643.
19 T. Yoshimura, A. Sakato, K. Tsuchiya, T. Ohkubo, H. Sakai, M. Abe and K. Esumi, *J. Colloid Interface Sci.*, 2007, **308**, 466.
20 K. Sakai, S. Umezawa, M. Tamura, Y. Takamatsu, K. Tsuchiya, K. Torigoe, T. Ohkubo, T. Yoshimura, K. Esumi, H. Sakai and M. Abe, *J. Colloid Interface Sci.*, 2008, **318**, 440.
21 T. Yoshimura, M. Bong, K. Matsuoka, C. Honda and K. Endo, *J. Colloid Interface Sci.*, 2009, **339**, 230.
22 K. Morishima, S. Sugawara, T. Yoshimura and M. Shibayama, *Langmuir*, 2017, **33**, 6084.
23 T. Morita, S. Yada and T. Yoshimura, *Langmuir*, 2022, **38**, 156.
24 T. Morita, S. Yada and T. Yoshimura, *Colloids Surf., A*, 2023, **671**, 131589.
25 T. Morita, S. Yada and T. Yoshimura, *Phys. Chem. Chem. Phys.*, 2023, **25**, 16288.
26 A. Einstein, *Ann. Phys.*, 1905, **322**, 549.
27 J. S. Pedersen, *Adv. Colloid Interface Sci.*, 1997, **70**, 171.
28 D. I. Svergun and M. H. J. Koch, *Rep. Prog. Phys.*, 2003, **66**, 1735.
29 D. Bendedouch, S. H. Chen and W. C. Koehler, *J. Phys. Chem.*, 1983, **87**, 2621.
30 J. B. Hayter and J. Penfold, *Mol. Phys.*, 1981, **42**, 109.
31 M. Kotlarchyk and S. H. Chen, *J. Chem. Phys.*, 1983, **79**, 2461.
32 J. P. Hansen and J. B. Hayter, *Mol. Phys.*, 1982, **46**, 651.
33 S. S. Berr, *J. Phys. Chem.*, 1987, **91**, 4760.

34 H. Rehage and H. Hoffmann, *J. Phys. Chem.*, 1988, **92**, 4712.
35 C. Tanford, *J. Phys. Chem.*, 1972, **76**, 3020.
36 Z. H. Asadov, G. A. Ahmadova, R. A. Rahimov, S. Z. F. Hashimzade, S. M. Nasibova, E. H. Ismailov, S. A. Suleymanova, S. A. Muradova, N. Z. Asadova and F. I. Zubkov, *Colloids Surf., A*, 2019, **575**, 212.
37 M. S. Bakshi, *Cryst. Growth Des.*, 2016, **16**, 1104.
38 R. Kaur, K. Singh, P. Khullar, A. Gupta, G. K. Ahluwalia and M. S. Bakshi, *Langmuir*, 2019, **35**, 14929.